A Generalized Framework for Process-informed Nonstationary Extreme Value Analysis

Elisa Ragno[a], Amir AghaKouchak[a], Linyin Cheng[b], Mojtaba Sadegh[c]

[a]*Department of Civil and Environmental Engineering, University of California, Irvine, USA.*
[b]*Department of Geosciences, University of Arkansas, Fayetteville, AR 72701, USA*
[c]*Department of Civil Engineering, Boise State University, ID, USA.*

Abstract

Evolving climate conditions and anthropogenic factors, such as CO_2 emissions, urbanization and population growth, can cause changes in weather and climate extremes. Most current risk assessment models rely on the assumption of stationarity (i.e., no temporal change in statistics of extremes). Most nonstationary modeling studies focus primarily on changes in extremes over time. Here, we present Process-informed Nonstationary Extreme Value Analysis (ProNEVA) as a generalized tool for incorporating different types of physical drivers (i.e., underlying processes), stationary and nonstationary concepts, and extreme value analysis methods (i.e., annual maxima, peak-over-threshold). ProNEVA builds upon a newly-developed hybrid evolution Markov Chain Monte Carlo (MCMC) approach for numerical parameters estimation and uncertainty assessment. This offers more robust uncertainty estimates of return periods of climatic extremes under both stationary and nonstationary assumptions. ProNEVA is designed as a generalized tool allowing using different types of data and nonstationarity concepts physically-based or purely statistical) into account. In this paper, we show a wide range of applications describing changes in: annual maxima river discharge in response to urbanization, annual maxima sea levels over time, annual maxima temperatures in response to CO_2 emissions in the atmosphere, and

---
*Corresponding Author
Email address: `ragnoe@uci.edu` (Elisa Ragno)

precipitation with a peak-over-threshold approach. ProNEVA is freely available to the public and includes a user-friendly Graphical User Interface (GUI) to enhance its implementation.

1. Introduction

Natural hazards pose significant threats to public safety, infrastructure integrity, natural resources, and economic development around the globe. In recent years, the frequency and impacts of extremes have increased substantially

5 in many parts of the world (e.g., Melillo et al., 2014; Coumou & Rahmstorf, 2012; Alexander et al., 2006; Mazdiyasni et al., 2017; Mallakpour & Villarini, 2017; Hallegatte et al., 2013; Wahl et al., 2015; Vahedifard et al., 2016; Jongman et al., 2014; AghaKouchak et al., 2014). For this reason, there is a great deal of interest in understanding how extreme events will change in the future.

10 Historical observations are the main source of information on extremes (Klemeš, 1974; Koutsoyiannis & Montanari, 2007) and statistical models are used to infer frequency and variability of extremes based on historical records (e.g., Katz et al., 2002).

Statistical models used to study extremes can be broadly categorized into

15 two groups: stationary and nonstationary (e.g., Salas & Pielke Sr, 2002; Coles & Pericchi, 2003; Griffis & Stedinger, 2007; Obeysekera & Salas, 2013; Serinaldi & Kilsby, 2015; Madsen et al., 2013; Koutsoyiannis & Montanari, 2015). In a stationary model, the observations are assumed to be drawn from a probability distribution function with constant parameters (i.e., statistics of extremes do

20 not change over time or with respect to another covariate). In a nonstationary model, however, the parameters of the underlying probability distribution function change over time or in response to a given covariate (Sadegh et al., 2015).

Water resources practices (e.g., flood and precipitation frequency analysis)

2

²⁵ have traditionally adopted stationary models. However, over the past decades, increasing surface temperatures (e.g., Barnett et al., 1999; Villarini et al., 2010; Melillo et al., 2014; Diffenbaugh et al., 2015; Fischer & Knutti, 2015; Mazdiyasni & AghaKouchak, 2015), more intense rainfall events (e.g., Zhang et al., 2007; Villarini et al., 2010; Min et al., 2011; Marvel & Bonfils, 2013; Westra et al.,

³⁰ 2013; Cheng et al., 2014; Fischer & Knutti, 2016; Mallakpour & Villarini, 2017), changes in river discharge (e.g., Villarini et al., 2009a,b; Hurkmans et al., 2009; Stahl et al., 2010), and sea level rise (e.g., Holgate, 2007; Haigh et al., 2010; Wahl et al., 2011) have been observed and to a great extent attributed to anthropogenic activities (e.g., human-caused climate change, urbanization).

³⁵ Matalas (1997) argued that trend in hydrological records cannot firmly be established because of the variables intrinsic variability and limited length of observations. In his reasoning, the observed trend might only be part of a slow oscillation. Consequently, Matalas (1997) defined hydrological trends as "real (physical)" or "perceived (statistical)". Even though using statistical trend

⁴⁰ analysis tools inevitably leads to detecting only statistical trends, it is important to make a distinction between a trend which has a physical explanation (e.g., increases in runoff in response to urbanization) and a trend which cannot be fully explained by our understanding of the underlying processes. Regardless of the type of observed hydrologic trends, i.e. in response to a physical process

⁴⁵ or only perceived (statistical), these trends challenge the stationary assumption (Milly et al., 2008).

Several studies have promoted the idea of moving away from stationary models to ensure capturing the changing properties of extremes (Milly et al., 2008). However, some have criticized this viewpoint particularly because the

⁵⁰ assumption of nonstationarity implies adding a deterministic component in the stochastic process, which must be justified by a well-understood process (Koutsoyiannis, 2011; Matalas, 2012; Lins & Cohn, 2011; Koutsoyiannis & Montanari, 2015). Moreover, limited observations could affect the exploratory diagnostics used to justify a nonstationary model (Serinaldi & Kilsby, 2015). This can

⁵⁵ potentially lead to higher uncertain in the results of extreme value analysis.

A nonstationary approach may also involve an assumption on the evolution of the relevant process/variable in the future which would add to the overall uncertainty (Serinaldi & Kilsby, 2015). When it is not possible to determine a credible prediction of the future Koutsoyiannis & Montanari (2015) or make a reasonable assumption, considering a stationary model may be a more appropriate solution. Luke et al. (2017) concluded that for prediction of river discharge, a stationary model should be preferred to avoid over-extrapolation in the future. However, when information about alterations occurred within a watershed is known, then an updated stationary model which accounts for the detected changes should be adopted (Luke et al., 2017). In the debate around model assumptions, Montanari & Koutsoyiannis (2014) noted that more efforts should focus on including relevant physical processes in stochastic models, and suggested stochastic-process-based models as a way to bridge the gap between physically-based models without statistics and statistical models without physics.

Here, we propose a generalized framework named *Process-informed Nonstationary Extreme Value Analysis* (ProNEVA) in which the nonstationarity component is defined by a temporal or process-based dependence of the observed extremes on an explanatory variable (i.e., a physical driver). Here, Process-informed refers to the process of incorporating a physical driver into a statistical analysis, when there is evidence that the physical driver can alter the statistics of the extremes. Even though the approach proposed is purely data-driven, it encourages and facilitates the implementation of informed statistical analysis in light of external knowledge of processes, especially for water resources management and risk assessment. For example, ProNEVA can be used for analyzing changes in extreme temperatures as a function of CO_2 emissions. It is widely recognized that higher amount of CO_2 in the atmosphere results in a warmer climate (e.g., Zwiers et al., 2011; Fischer & Knutti, 2015; Barnett et al., 1999). For this reason, CO_2 emissions can be considered a physical covariate for explaining temperature extremes. Other examples include temperature or large scale climatic circulations as covariates for rainfall, and CO_2 concentration or

4

temperature as covariates for sea level rise.

2. Background and Method

2.1. Nonstationarity Extreme Value Analysis

⁹⁰   Extreme Value Theory (EVT) provides the bases for estimating the magnitude and frequency of hazardous events (including natural and non-natural extreme events) (Coles, 2001). Most applications utilize either the Generalized Extreme Value distribution (GEV) or the Generalized Pareto distribution (GP) for describing the behavior of extremes. The former is applied to the
⁹⁵   annual maxima of a variable (e.g., a time series consisting of the most extreme daily rainfall from each year of the record), while the latter is used to describe extremes above a predefined threshold (e.g., all independent river flow values above the flood stage). Both GEV and GP allow incorporating nonstationarity through varying parameters. Several studies have investigated methodologies
¹⁰⁰   for testing the assumptions of stationarity and nonstationarity in hydrology, climatology, and earth system sciences (e.g., Katz et al., 2002; Sankarasubramanian & Lall, 2003; Cooley et al., 2007; Mailhot et al., 2007; Huard et al., 2009; Villarini et al., 2009a; Towler et al., 2010; Villarini et al., 2010; Vogel et al., 2011; Salas et al., 2012; Zhu et al., 2012; Willems et al., 2012; Katz, 2013; Obeysekera
¹⁰⁵   & Salas, 2013; Salas & Obeysekera, 2014; Rosner et al., 2014; Yilmaz & Perera, 2014; Mirhosseini et al., 2014; Cheng & AghaKouchak, 2014; Steinschneider & Lall, 2015; Volpi et al., 2015; Krishnaswamy et al., 2015; Read & Vogel, 2015; Sadegh et al., 2015; Mirhosseini et al., 2015; Mondal & Mujumdar, 2015; Lima et al., 2015, 2016b,a; Sarhadi & Soulis, 2017; Salas et al., 2018; Yan et al., 2018;
¹¹⁰   Bracken et al., 2018; Ragno et al., 2018).

A number of packages and software tools are currently available for nonstationary Extreme Value Analysis (EVA), including the R-package *ismev* (Gilleland et al., 2013; Gilleland & Katz, 2016) where nonstationarity is modeled as a linear regression function of generic covariates (Gilleland et al., 2013). *extRemes*
¹¹⁵   offers EVA capability and evaluates the underlying uncertainties with respect

to parameters (Gilleland & Katz, 2016). *extRemes* also allows tail-dependence analysis and a declustering technique for peak over threshold analysis. The package *climextRemes* (available also in Python) builds upon *extRemes* and includes an estimate of the risk ratio for event attribution analyses. R packages

120 *vgam* and *gamlss* are available for modeling nonstationarity through generalized additive models (see for example Villarini et al. (2009a)). The package *GEVcdn* estimates the parameters of a nonstationary GEV distribution using a conditional density method (Cannon, 2010).

Cheng et al. (2014) developed a Bayesian-based framework, *Nonstationary*

125 *Extreme Value Analysis* (NEVA) toolbox that estimates the parameters of GEV and GP distributions and their associated uncertainty for time-dependent extremes (available in Matlab). In the nonstationary case, the parameters are modeled as a linear function of time. NEVA also includes return level curves based on the concept of expected waiting time (Wigley, 2009; Olsen et al., 1998;

130 Salas & Obeysekera, 2014) and effective return level (Katz et al., 2002). The package *nonstationary Flood Frequency Analysis* estimates the parameters of the Log-Pearson Type III distribution as a linear function of time, based on Bayesian inference approach (Luke et al., 2017). The *tsEVA* toolbox implements the Transformed-Stationary (TS) methodology described in Mentaschi

135 et al. (2016), which comprises of, first, a transformation of a nonstationary time series into a stationary one, so that the stationary EVA theory can be applied, and then a reverse-transformation of the results to include the nonstationary components in the GEV and the GP distributions.

Despite significant advances, a comprehensive framework which incorporates

140 the widely used EVA statistical models, namely GP, GEV, and LP3, under both stationary and nonstationary assumptions (parameters as a function of time or a physical covariates) is not available. Moreover, the implementation of newly proposed approaches for return period estimation under the nonstationary assumption is still limited. To address the above limitations, we present

145 ProNEVA, which builds upon NEVA package (Cheng et al., 2014) but expands to a general nonstationary extreme value analysis. Indeed, in addition to station-

ary EVA, ProNEVA allows nonstationary analyses using user-defined covariates, which could be time or a physical variable. Figure 1 depicts the core structure of ProNEVA. The advantage of performing stationary analysis with physical-

150 related covariates resides in the possibility of imposing physical constraints to a statistical model. Even though such a statistical model (nonstationary statistical model) is purely data-driven, it can be constrained using physical information to avoid unrealistic extrapolation.

ProNEVA offers parameter estimation, uncertainty quantification, and a

155 comprehensive assessment of the goodness of fit. The key features of ProNEVA are described as follows: (a) the model includes the most common distribution functions used for extreme value analysis including the GEV, GP, and LP3 distributions; (b) for nonstationary analysis, the users can select both the covariate and the choice of function for describing change in parameters; (c) the covariate

160 can be any user-defined physical covariate; (d) the model also includes a default time-covariate (i.e., describing change over time without a physical covariate); (e) the function describing change in parameters with respect to the covariate can be linear, exponential, or quadratic; (f) the users can select the GP distribution threshold (peak-over-threshold) as a constant value or as a linear

165 quantile regression function of the choice covariate; (g) ProNEVA estimates the distribution parameters based on a Bayesian inference approach; (h) the model allows using a wide range of priors for parameters including the uniform, normal, and gamma distributions; (i) ProNEVA samples the posterior distribution function of the parameters using a newly-developed hybrid evolution Markov Chain

170 Monte Carlo (MCMC) approach, which is computationally more efficient than traditional MCMC algorithms searching rugged response surfaces and it provides a robust numerical parameter estimation and uncertainty quantification (Sadegh et al., 2017); (j) different model diagnostics and model selection indices (e.g., RMSE, AIC, BIC) are implemented to provide supporting information; (k)

175 ProNEVA includes exploratory data analysis tools such as the Mann-Kendall test for monotonic trends and the White test for homoscedasticity in time series; (l) in addition to the source code, a Graphical User Interface (GUI) for

7

ProNEVA is also available for easier implementation (see Supplementary Material); finally, (m) ProNEVA is intended for a broad audience and hence it is structured such that users can easily customize and modify it based on their needs. We acknowledge that there are other EVA methods, such as those in Serago & Vogel (2018) and Gilleland & Katz (2016), that we have not included in ProNEVA.

In the reminder of the paper, a detailed description of ProNEVA is provided. Four different example applications are presented with different variables (e.g., precipitation, sea level, temperature, river discharge) and different covariates (time, CO_2 emissions in the atmosphere, urbanization). ProNEVA can be used for analyzing annual maxima (also known as block maxima) using the GEV and LP3 distributions, and peak over threshold (POT) or partial duration series using the GP distribution. In the following, we provide a brief overview of the extreme value models and their parameters.

2.2. Generalized Extreme Value (GEV)

The GEV distribution function is used to model time series of block maxima. The National Oceanic and Atmospheric Administration (NOAA), for example, derives precipitation Intensity-Duration-Frequency (IDF) curves based on the GEV distribution. This distribution is also widely used in other fields including finance, seismology, and reliability assessment (bridge performance assessment (e.g., Ming et al., 2009)). The GEV cumulative distribution function is (Coles, 2001):

$$\Psi_{GEV}(x) = exp\Big\{ - \Big(1 + \xi \cdot \Big(\frac{x - \mu}{\sigma}\Big)\Big)^{-\frac{1}{\xi}}\Big\} \tag{1}$$

for $\xi \cdot \Big(\frac{x-\mu}{\sigma}\Big) > 0$. μ, σ, and ξ are the parameters of the distribution: μ is the location parameter, $\sigma > 0$ is the scale parameter, and ξ is the shape parameter which defines the tail behavior of the distribution.

The stationary GEV model can be extended for dependent series by letting the parameters of the distribution be a function of a general covariate x_c, i.e., $\mu(x_c)$, $\sigma(x_c)$, $\xi(x_c)$, (Coles, 2001). Hence, the nonstationary form of eq. 1 is
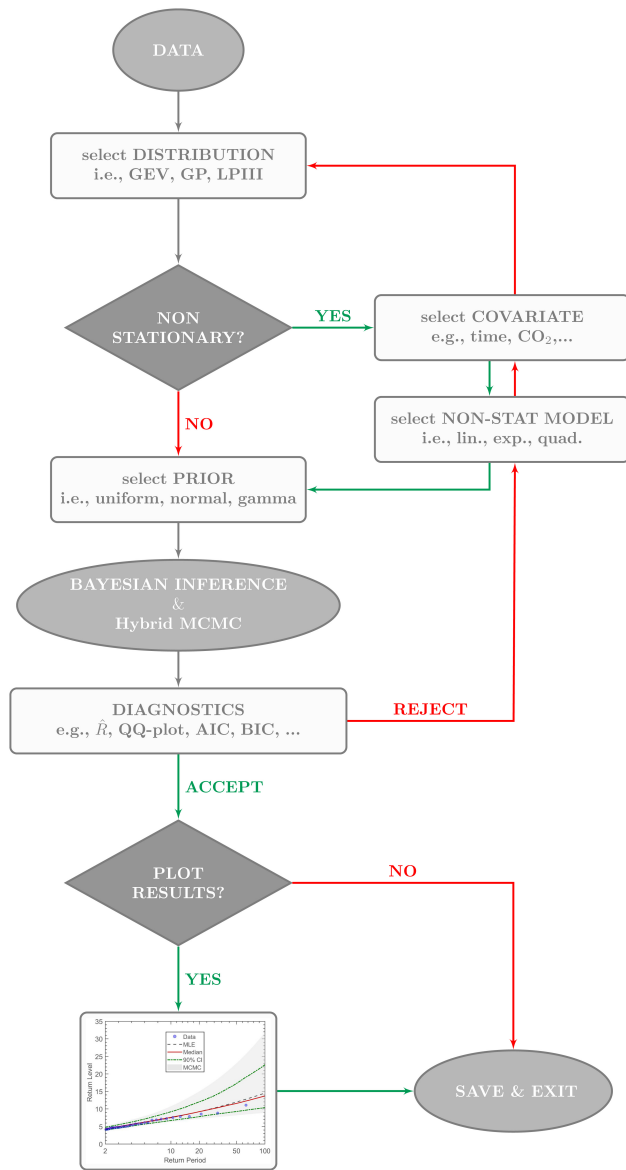
8

Figure 1: Flowchart representing the core structure of the Matlab Toolbox ProNEVA

described as:

$$\Psi_{GEV}(x|x_c) = exp\Big\{ - \Big(1 + \xi(x_c) \cdot \Big(\frac{x - \mu(x_c)}{\sigma(x_c)}\Big)\Big)^{-\frac{1}{\xi(x_c)}} \Big\} \qquad (2)$$

In ProNEVA, for each of the three parameters, the users can select a function to describe the change in the parameters with respect to the covariate x_c (Table S1 - Supplementary Material). The function selected for each parameter does not constrain the functional relationship used for the other parameters. To ensure the positivity of the scale parameter, $\sigma(x_c)$ is modeled in the log-scale (Coles, 2001; Katz, 2013). Consequently, the exponential function is not available for $\sigma(x_c)$. Moreover, the shape parameter $\xi(x_c)$ is known to be a difficult parameter to precisely estimate even in the stationary case, (Coles, 2001), especially for short time series, (Papalexiou & Koutsoyiannis, 2013). For this reason, only the linear function is included for $\xi(x_c)$.

2.3. Generalized Pareto (GP)

The GP distribution is used for modeling time series sampled based on the POT method. The GP distribution has been applied to precipitation (e.g., De Michele & Salvadori, 2003), earthquake data (e.g., Pisarenko & Sornette, 2003), wind speed (Holmes & Moriarty, 1999), and economic data (e.g., Gençay & Selçuk, 2004), among others. Given a sequence Y of independent and random variables, for a large enough threshold u, the cumulative distribution function of the excesses $Y_e = Y - u$, conditional on $Y > u$, is approximated by the GP distribution function, (Coles, 2001):

$$\Psi_{GP}(y_e) = 1 - \Big(1 + \xi \cdot \Big(\frac{y_e}{\sigma}\Big)\Big)^{-\frac{1}{\xi}} \qquad (3)$$

In particular, if block maxima of Y follows a GEV distribution, then the threshold excesses Y_e have a GP distribution in which the parameter ξ is equal to the parameter ξ of the corresponding GEV distribution (Coles, 2001).

In the nonstationary model of the GP distribution, both the threshold value and the parameters of the distribution can be modeled as a function of the

10

user-covariate x_c, (Coles, 2001).

$$\Psi_{GP}(y_e|x_c) = 1 - \left(1 + \xi(x_c) \cdot \left(\frac{y_e(x_c)}{\sigma(x_c)}\right)\right)^{-\frac{1}{\xi(x_c)}} \tag{4}$$

Where $Y_e(x_c) = Y - u(x_c)$. Analogous to the GEV case, ProNEVA allows incorporating different functional forms for describing change in parameters over time or with respect to a covariate (Table S2).

The same considerations for the GEV parameter functional forms are applied to GP distribution too. In addition, the users can specify the type of threshold u. Two quantile-based options are available: constant or linear. In the case of a linear threshold, a linear regression quantile model is adopted. The α-regression quantile function is (Koenker & Bassett, 1978; Kyselý et al., 2010)

$$\tilde{\mathbf{Y}} = \mathbf{M} \cdot \mathbf{U}(\alpha) + \mathbf{r}^+ - \mathbf{r}^- \tag{5}$$

where $0 < \alpha < 1$ is the quantile, $\tilde{\mathbf{Y}}$ is the column vector of n-observations, $\mathbf{M} = [\, \mathbf{X_c} \quad \mathbf{I_n} \,]$ with $\mathbf{X_c}$ being the column vector of covariance and $\mathbf{I_n}$ the n-identity vector, $\mathbf{U} = [\, u_1 \quad u_0 \,]'$ is the vector of the regression coefficients, and $\mathbf{r}^+$ and $\mathbf{r}^-$ are respectively the positive and negative parts of the residuals. Then, $\mathbf{U}(\alpha)$ is calculated as the optimal solution to eq. 6 (Koenker & Bassett, 1978; Kyselý et al., 2010).

$$\alpha \cdot \mathbf{I_n}' \cdot \mathbf{r}^+ + (1 - \alpha) \cdot \mathbf{I_n}' \cdot \mathbf{r}^- := min \tag{6}$$

2.4. Log-Pearson Type III (LP3)

The LP3 distribution has been widely used in hydrology for flood frequency analysis particularly after the release of the USGS Bulletin 17B (U.S. Water Resources Council, 1982). However, it has been applied to other studies, such as design magnitude of earthquakes (Gupta & Deshpande, 1994) and evaluation of apple bud burst time and frost risk (Farajzadeh et al., 2010).

The LP3 distribution characterizes the random variable $Q = exp(X)$, given that X follows a Pearson type III (P3) distribution (Griffis et al., 2007). Hereafter, the natural logarithm is used, however any base can be implemented, such

as base-10 as in Bulletin 17B (Griffis et al., 2007). The P3 probability density function is

$$\psi_{P3}(x) = \frac{1}{|\beta| \cdot \Gamma(\alpha)} \cdot \left(\frac{x - \tau}{\beta}\right)^{\alpha - 1} \cdot \exp\left(-\frac{x - \tau}{\beta}\right) \tag{7}$$

defined for $\alpha > 0$, $(x - \tau)/\beta > 0$, and $\Gamma(\alpha)$ being a complete gamma function (Griffis et al., 2007). The parameters α, β, and τ are functions of the first three moments, μ_X, σ_X, γ_X, (Griffis et al., 2007):

$$\alpha = 4/\gamma_X^2 \tag{8}$$

$$\beta = (\sigma_X \cdot \gamma_X)/2 \tag{9}$$

$$\tau = \mu_X - 2 \cdot (\sigma_X/\gamma_X) \tag{10}$$

In the case of nonstationary analysis, the first three moments are modeled as a function of the user-defined covariate x_c (Table S3). The GEV and GP considerations mentioned above hold for the functions to describe change in parameters.

$$\psi_{P3}(x|x_c) = \frac{1}{|\beta(x_c)| \cdot \Gamma(\alpha(x_c))} \cdot \left(\frac{x - \tau(x_c)}{\beta(x_c)}\right)^{\alpha(x_c) - 1} \cdot \exp\left(-\frac{x - \tau(x_c)}{\beta(x_c)}\right) \tag{11}$$

3. Parameter Estimation: Bayesian Analysis and Markov Chain Monte Carlo Sampling

ProNEVA estimates the parameters of the selected (non)stationary EVA distribution using a Bayesian approach, which provides a robust characterization of the underlying uncertainty derived from both input errors and model selection. Bayesian analysis has been widely implemented for parameter inference and uncertainty quantification (e.g. Thiemann et al., 2001; Gupta et al., 2008; Cheng et al., 2014; Kwon & Lall, 2016; Sarhadi et al., 2016; Sadegh et al., 2017; Luke et al., 2017; Sadegh et al., 2018).

Let θ be the parameter of a given distribution and let $\tilde{\mathbf{Y}} = \{\tilde{y}_1, \ldots, \tilde{y}_n\}$ be the set of n observations. Following Bayes theorem, the probability of θ given $\tilde{\mathbf{Y}}$ (posterior) is proportional to the product of the probability of θ (prior) and the probability of $\tilde{\mathbf{Y}}$ given θ (likelihood function). Assuming independence between the observations:

12

$$p(\theta|\tilde{\mathbf{Y}}) \propto \prod_{i=1}^{n} p(\theta) \cdot p(\tilde{y}_i|\theta) \tag{12}$$

The prior brings a priori information, which does not depend on the observed data, into the parameter estimation process. The choice of the prior distribution, then, is subjective, and it is based on prior beliefs about the system of interest (Sadegh et al., 2018). The available prior options in ProNEVA include the uniform, normal, and gamma distributions, providing a variety of possibilities. ProNEVA assumes independence of parameters and hence, each parameter requires its own prior.

In the case of a nonstationary analysis, the vector of parameters θ includes a higher number of elements than in the stationary case, depending on the functional form selected for each of the distribution's parameters.

The posterior distribution is then delineated using a hybrid-evolution MCMC approach proposed by Sadegh et al. (2017). The MCMC simulation searches for the region of interest with multiple chains running in parallel, which share information on the fly. Moreover, the hybrid-evolution MCMC benefits from an intelligent starting point selection (Duan et al., 1993) and employs Adaptive Metropolis (AM) (Roberts & Sahu, 1997; Haario et al., 1999, 2001; Roberts & Rosenthal, 2009), differential evolution (DE) (Storn & Price, 1997; Ter Braak & Vrugt, 2008; Vrugt et al., 2009), and snooker update (Gilks et al., 1994; Ter Braak & Vrugt, 2008; Sadegh & Vrugt, 2014) algorithms to search the feasible space. The Metropolis ratio is selected to accept/reject the proposed sample, and the Gelman-Rubin $\hat{R}$ (Gelman & Rubin, 1992) is selected to monitor the convergence of the chains, which should remain below the critical threshold of 1.2. For a more detailed description of the algorithm, the reader is referred to Sadegh et al. (2017).

4. Model Diagnostics and Selection

The purpose of fitting a statistical model, whether it is stationary or nonstationary, is to characterize the population from which the data was drawn

for further analysis/inference (Coles, 2001). Hence, it is necessary to check the

305 performance of the fitted model to the data (Coles, 2001). We implemented different metrics in the ProNEVA for goodness of fit (GOF) assessment and model selection including: quantile and probability plots for a graphical assessment (see Supplementary Material), two-sample Kolmogorov-Smirnov (KS) test, Akaike Information Criterion (AIC), Bayesian Information Criterion (BIC), Maximum

310 Likelihood (ML), Root Mean Square Error (RMSE), and Nash-Sutcliff Efficiency (NSE) coefficient. The hybrid-evolution MCMC approach (Sadegh et al., 2017) within the Bayesian framework provides an ensemble of solutions for the (non)stationary statistical model fitted to the data. ProNEVA uses the best set of parameters, $\hat{\theta}$, which maximizes the posterior distribution. Marginal poste-

315 riors will then provide uncertainty estimates of the estimated parameters.

4.1. Standard Transformation

When applied to nonstationary applications, the lack of homogeneity in the distributional assumption requires an adjustment to the traditional GOF techniques (Coles, 2001). Consequently, ProNEVA standardizes the observations

320 based on the underlying distribution family such that the GOF tests can be performed. Table S4 provides information on the transformation methods in ProNEVA. However, it is worth noting that the choice of the reference distribution is arbitrary (Coles, 2001). Here, we selected those transformations that are widely accepted in the literature (Coles, 2001; Koutrouvelis & Canavos, 1999).

325 In the case of a LP3 distribution, the transformation can only be applied when the parameter α is constant (Koutrouvelis & Canavos, 1999). Based on eq. 8, this implies that the transformation can be performed only in the case of constant skewness γ_X.

4.2. Kolmogorov-Smirnov Test

330 The two-sample Kolmogorov-Smirnov (KS) test is a non-parametric hypothesis testing technique which compares two samples, $Z^{(1)}$ and $Z^{(2)}$, to assess whether they belong to the same population (Massey, 1951). Being $F_{Z^{(1)}}(z)$

and $F_{Z^{(2)}}(z)$ the (unknown) statistical distributions of $Z^{(1)}$ and $Z^{(2)}$ respectively, the null-hypothesis H_0 is $F_{Z^{(1)}}(z) = F_{Z^{(2)}}(z)$, against alternatives. The
KS test statistic D^* is:

$$D^* = \max_z(|F_{Z^{(1)}}(z)) - F_{Z^{(2)}}(z)|) \tag{13}$$

H_0 is rejected when the p_{value} of the test is equal to or exceeds the selected α-level of significance, e.g., 5%. We implemented the KS test in ProNEVA as one of the methods to test the goodness-of-fit of the model. Specifically, ProNEVA generates 1000 random samples from the fitted statistical distribution or, in the case of a nonstationary analysis, from the reference distribution. Then, the KS test is performed between the random samples and the input (original or transformed) data. Finally, the rejection rate (RR), eq. 14, is provided as a GOF index.

$$RR = \frac{\sum(H_0 \quad rejected)}{1000} \tag{14}$$

4.3. Model Selection based on Model Complexity

A model showing desirable level of performance efficiency with the minimum number of parameters, i.e., a parsimonious model (Serago & Vogel, 2018), is usually preferred over a model with similar performance but more parameters - e.g, a nonstationary model with more parameters relative to a simpler stationary model (Serinaldi & Kilsby, 2015; Luke et al., 2017). Consequently, ProNEVA evaluates different GOF metrics (i.e., AIC, BIC), which account for the number of parameters within the numerical model.
The Akaike Information Criterion (AIC) (Akaike, 1974, 1998; Aho et al., 2014) is formulated as follows

$$AIC = 2 \cdot (D - \hat{L}) \tag{15}$$

where D is the number of parameters of the statistical model and $\hat{L}$ is the log-likelihood function evaluated at $\hat{\theta}$. The model associated with a lower AIC is considered a better fit.

The Bayesian Information Criterion (BIC) (Schwarz, 1978) is defined as

$$BIC = D \cdot ln(N) - 2 \cdot \hat{L} \tag{16}$$

15

where N is the length of records. Similar to AIC, the model with lower BIC results a better fit.

4.4. Model Selection based on Minimum Residual

Root Mean Square Error (RMSE) and Nash-Sutcliff Efficiency (NSE) coefficient are two metrics widely used in hydrology and climatology as GOF measurements (Sadegh et al., 2018). The focus of both is to minimize the residuals. The vector of residual is defined as

$$\mathbf{RES} = \left(\left(\hat{F}^{-1}\left(\frac{1}{n+1}\right) - z_{(1)} \right), \cdots, \left(\hat{F}^{-1}\left(\frac{i}{n+1}\right) - z_{(i)} \right), \cdots, \left(\hat{F}^{-1}\left(\frac{n}{n+1}\right) - z_{(n)} \right) \right); \tag{17}$$

following the same notation used for defining the quantile plot. Hence,

$$RMSE = \sqrt{\frac{\sum_{i=1}^{n} RES_i^2}{n}} \tag{18}$$

$$NSE = 1 - \frac{\sum_{i=1}^{n} RES_i^2}{\sum_{i=1}^{n} (z_{(i)} - mean(z))^2} \tag{19}$$

A perfect fit is associated with $RMSE = 0$ and $NSE = 1$, given $RMSE \in [0, \inf)$ and $NSE \in [-\inf, 1)$.

5. Predictive Distribution

The primary objective of a statistical inference is to predict unobserved events (Renard et al., 2013). EVA, for example, provides the basis for estimating loads for infrastructure design and risk assessment of natural hazards (e.g., floods, extreme rainfall events). Considering a Bayesian viewpoint, the predictive distribution can be written as (Renard et al., 2013):

$$f(\mathbf{z}|\tilde{\mathbf{Y}}) = \int f(\mathbf{z}, \theta|\tilde{\mathbf{Y}}) \cdot d\theta = \int f(\mathbf{z}|\theta) \cdot f(\theta|\tilde{\mathbf{Y}}) \cdot d\theta \tag{20}$$

where $\tilde{\mathbf{Y}}$ is the observed data, $\mathbf{z}$ is a grid at which $f(\mathbf{z}|\tilde{\mathbf{Y}})$ will be evaluated, θ is the vector of parameters, $f(\mathbf{z}|\theta)$ is the probability density function (pdf) of the selected distribution (i.e., GEV, GP, LP3), and $f(\theta|\tilde{\mathbf{Y}})$ is the posterior distribution function. The predictive distribution function relies on the fitted

16

distribution function over the parameter space, and uses the posterior distribution for uncertainty estimation (Renard et al., 2013). In practice, eq. 20 often cannot be derived analytically. Therefore, Renard et al. (2013) suggest to numerically evaluate it using the MCMC-derived ensemble of solutions sampled from the posterior distribution. The probability density of the k_{th}-element of the vector $\mathbf{z}$ is:

$$\hat{f}(z_k|\tilde{\mathbf{Y}}) = \frac{1}{N_{sim}} \cdot \sum_{i=1}^{N_{sim}} f(z_k|\theta_i) \qquad (21)$$

In the nonstationary case, the predictive pdf is a function of the covariate, since the distribution parameters depend on the covariates. For this reason, ProNEVA provides the predictive pdf for a number of predefined values of the covariates.

6. Return Level Curves under Nonstationarity

Given a time series of annual maxima, the Return Level (RL) is defined as the quantile Q_i for which the probability of an annual maximum exceeding the selected quantile is q_i (Cooley, 2013). For example, let's assume that annual maxima of precipitation intensities $P = p_1, \cdots, p_n$ have probability distribution F_P. The quantile Q_i is the value of precipitation intensity such that $Pr(P \geq Q_i) = 1 - F_P(Q_i) = q_i$. Under the stationary assumption, the characteristics of the statistical model are constant over time, meaning that the probability q_i of the quantile Q_i does not change on a yearly basis. In this context, the concept of Return Period (RP) of the quantile Q_i is defined as the inverse of its exceedance probability, $T_i = 1/q_i$ in years. Referring back to the example of annual maxima of precipitation intensities P, let's assume that Q_i is the precipitation intensity quantile such that the probability of being exceeded in each given year is $Pr(P \geq Q_i) = 1 - F_P(Q_i) = 0.01$. Then, the RP of Q_i (or RL) is $T_i = 1/q_i = 1/0.01 = 100$ in years. Under the stationary assumption, there is a one-to-one relationship between RL and RP (Cooley, 2013). Therefore, the RL curves are defined by the following points:

$$\left(\left(T_i; Q_i \right), \quad T_i > 1 \quad yr, \quad i = 1, \cdots \right) \qquad (22)$$

17

RL curves are traditionally used for defining extreme design loads for infrastructure design and risk assessment of natural hazards. However, in a nonstationary context both RP and RL terms become ambiguous (Cooley, 2013) and numerous studies have attempted to address the issue. For nonstationary analysis, ProNEVA integrates two different proposed concepts: the expected waiting time (Salas & Obeysekera, 2014), for default time-covariate only, and the effective RL curves (Katz et al., 2002).

6.1. Effective Return Level

Katz et al. (2002) proposed the concept of effective design value (or effective return level), which is defined as q-quantile, Q, varying as a function of a given covariate (i.e, time or physical). Therefore, for a constant value of $RP = 1/q$, where q is the yearly exceedance probability, the effective RL curves is defined by the points

$$\left(\left(x_c, Q_q(x_c) \right), \quad q \in [0, 1] \right) \tag{23}$$

where x_c is the covariate, and $Q_q(x_c)$ is the q-quantile.

6.2. Expected Waiting Time

Wigley (2009) first introduced the concept of waiting time, i.e., the expected waiting time until an event of magnitude Q_i is exceeded, in which the probability of exceedance in each year, q_i, changes over time. Olsen et al. (1998) and, later, Salas & Obeysekera (2014) provided a comprehensive mathematical description of the suggested concept.

The event Q_{q_0} is defined as the event with the exceedance probability at time $t = 0$ equal to q_0. Under nonstationary conditions, at time $t = 1$ the probability of exceedance of Q_{q_0} will be q_1, at time $t = 2$, it will be q_2, and so on. Given the selected statistical model F_Q with characteristics θ_t, $q_t = 1 - F_Q(Q_{q_0}, \theta_t)$. Hence, the probability of the event to exceed Q_{q_0} at time m is given by (Salas & Obeysekera, 2014):

$$f(m) = q_m \cdot \prod_{t=1}^{m-1} (1 - q_t) \tag{24}$$

18

where $f(1) = q_1$ and $f(m) = 1$. The cumulative distribution function (cdf) of a geometrical distribution (eq. 24) is:

$$F_X(x) = \sum_{i=1}^{x} f(i) = \sum_{i=1}^{x} q_i \cdot \prod_{t=1}^{i-1}(1 - q_t) = 1 - \prod_{t=1}^{x}(1 - q_t) \qquad (25)$$

where x is the time at which the event occurs, $x = 1, \cdots, x_{max}$, $F_X(1) = q_1$, and $F_X(x_{max}) = 1$. Therefore, the expected waiting time (or RP) in which for the first time the occurring event exceeds Q_{q_0} can be derived as

$$T = E(X) = \sum_{x=1}^{x_{max}} x \cdot f(x) = \sum_{x=1}^{x_{max}} x \cdot p_x \prod_{t=1}^{x-1}(1 - p_t) \qquad (26)$$

Cooley (2013) simplifies eq. (26) as:

$$T = E(X) = 1 + \sum_{x=1}^{x_{max}} \prod_{t=1}^{x}(1 - p_t) \qquad (27)$$

which gives the return period under nonstationary conditions, and it is consistent with the definition of RP in the stationary case (Salas & Obeysekera, 2014).

7. Explanatory Analysis: Mann-Kendall and White Tests

With the intention of providing explanatory data analysis, ProNEVA includes two different tests: the Mann-Kendall (MK) monotonic trend test and the White Test (WT) for evaluating homoscedasticity in the records. These tests can be used to decide whether to incorporate a trend function in one or more of the model parameters or not (i.e., deciding whether to use a stationary or nonstationary model). However, these tests are optional and are not an integral part of ProNEVA. The selection of a stationary versus a nonstationary analysis is untied from the tests results, but it is left to the users. For more details about the MK and WT, the readers is referred to the Supplementary Material and the references therein.

8. ProNEVA Graphical User Interface (GUI)

The framework here presented has also a Graphical User Interface (GUI), Figure 2, which we believe can promote and facilitate the application of ProNEVA. The User Manual included in the package will provide the user with all the instructions needed.
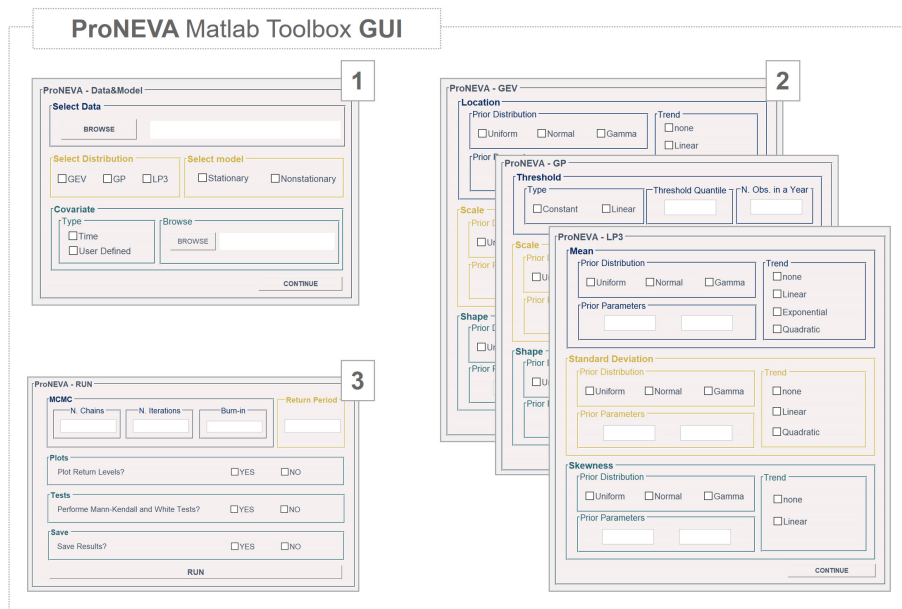

Figure 2: ProNEVA Graphical User Interface (GUI). 1) Interface for uploading data and selecting the choice of distribution (GEV/GP/LP3) and model (stationary/nonstationary) type; 2) Interface specific to the choice of distribution for selecting priors and nonstationarity model; 3) Interface for selecting MCMC information and additional operations (e.g., additional exploratory analyses, saving results, plotting options).

9. Results

As previously discussed, the changes in extremes observed over the past years can stem from changes in different physical processes. In order to account for the observed changes, we need statistical tools that are able to incorporate those variables causing variability, which can be represented as time-covariate

or a physical-based covariate. In the following, we show example applications of ProNEVA under both stationay and nonstationary assumptions including modeling changes induced by different types of covariates (both temporal and process-based changes). It is important to point out that for statistical analyses, under both the stationary and nonstationary assumptions, the quality of information (i.e., length of record, representativeness of observations), is fundamental. Generally, the more information is available, the more confident we can be about our inferences (and also whether or not a model is representative for the application in hand). However, often observations of extremes are limited. The issue of data quality and availability of covariates is also as important for nonstationary analysis. For all application, representativeness of the choice of model should be rigorously tested using different goodness-of-test methods.

In the first application, we analyze discharge data from Ferson Creek (St. Charles, IL), which has experienced intense urban development over the years. Urbanization has a direct effect on the amount of water discharged at the catchment outlet, since it increases impervious surfaces. For this reason, we use a process-informed nonstationary LP3 model for fitting discharge data, in which the covariate is represented by percent of urbanized catchment area. The second application involves temperature maxima data averaged over the Contiguous United States. Many studies have shown that the amount of CO_2 in the atmosphere causes temperatures to increase. For this reason, we fit a nonstationary GEV model to temperature data, in which the covariate is represented by CO_2 emissions in the atmosphere to include the underlying physical relationship. In the third application, we investigate sea level annual maxima in the city of Trieste (Italy), which has increased over the years. In this case, we adopted a temporal nonstationary GEV model. The last application involves precipitation data for New Orleans, Louisiana, in which we fit a stationary GP model, given that there is no evidence of change in statistics of extremes.

490   *9.1. Application 1: Modeling discharge with urbanization as the physical driver*

Since 1980, Ferson Creek (St. Charles, IL) basin has experienced land use land cover changes due to urbanization. The percent of urban areas within the catchment has increased from 20% of the total basin's area in 1980 to almost 65% in 2010. River discharge highly depends on the land use and land cover
495   of the basin as it determines the ratio of infiltration to direct runoff (Figure 3). Here, urbanization can be considered as a known physical process that has altered the runoff in the basin. To incorporate the known physical process, we investigate annual maxima discharge of the Ferson Creek (station USGS 05551200) using a process-informed nonstationary LP3 model, in which the covariate, x_c, is the percent of urbanized area. LP3 is widely used for modeling
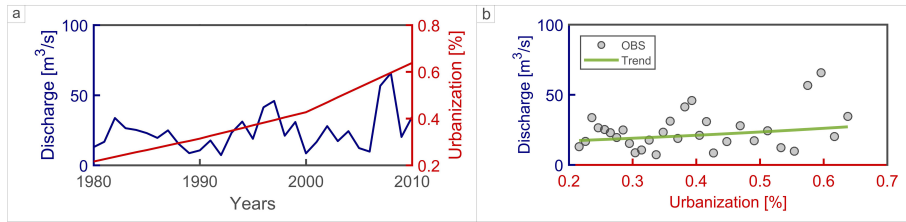
Figure 3: Application 1: Modeling discharge in Ferson Creek with urbanization as the physical driver of change. a) Discharge data and percent of urbanization in the basin; b) Discharge data as a function of urbanization.

500

discharge data (Bulletin 17B, U.S. Water Resources Council (1982)). We select a nonstationary model in which the parameter μ is an exponential function of the covariate x_c. We adopt normal priors for the LP3 parameters. Figure 4.b shows the results of the process-informed nonstationary analysis for an arbitrary value
505   of urbanized area, here 37%. For the sake of comparison, Figure 4.a displays the results when a stationary model is implemented. It is worth noting that the nonstationary model (Figure 4.b) fits extreme discharge values (high values of return period) better than the stationary model (Figure 4.a). While based on the AIC and BIC diagnostic tests, the stationary model and the nonstationary
510   model perform rather similarly, the RMSE of the nonstationary model (25.06 m^3/s) is considerably lower than that of the stationary model (77.58 m^3/s).
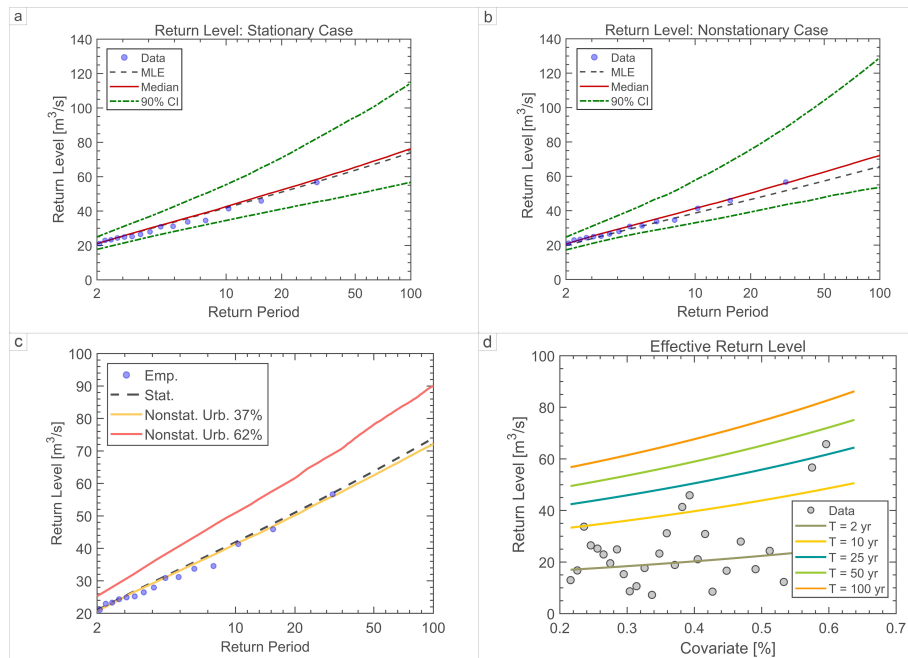
22

Figure 4: ProNEVA results for Application 1: Modeling discharge in Ferson Creek with urbanization as the physical driver of change. a) Return Level curves based on a stationary model; b) Return Level base on a nonstationary model considering an urbanization area equal to 37% of the catchment area; c) Expected return level curves, i.e. ensemble medians, under stationary and nonstationary assumption; d) Effective return period, i.e. return period as a function of the percent of urbanized area.

Urbanization alters the runoff in the basin by reducing the amount of water that infiltrates and increasing the amount of direct runoff. Figure 4.c shows the ability of the statistical model to incorporate this physical process. As anticipated, the expected (ensemble median) nonstationary return level curve associated with a 62% of urbanized area returns higher values of discharge than the one associated with a 37% of urbanized area. For example, under the nonstationary assumption, the magnitude of a 50-year event is 62.47 m^3/s for 37% of urbanized area, similar to the stationary case. However, the magnitude of the 50-year event increases to 78.11 m^3/s (25% more) for 62% of urbanized area. On the contrary, the stationary analysis estimates a 50-year event as an event with magnitude 63.74 m^3/s, independent of the level of urbanization of the catchment. The result demonstrates that a combination between statistical concepts and physical processes is required for correctly estimating the expected magnitude of an event. Figure 4.d displays the effective return level curves (Katz et al., 2002) which summarize the impact of urbanization on discharge by describing return levels as functions of the selected covariate (x-axis).

9.2. Application 2: Modeling temperature with CO_2 as the physical covariate

Over the past decades, many studies have reported increasing surface temperature (e.g.: Zhang et al., 2006; Stott et al., 2010; Melillo et al., 2014; Zwiers et al., 2011), mainly due to anthropogenic activities as a consequence of increase in greenhouse gasses concentration in the atmosphere. Therefore, we investigate annual maxima surface temperature for the Contiguous United States available from NOAA (NCDC archive - `https://www.ncdc.noaa.gov/cag/national/time-series`) using a process-informed nonstationary GEV model in which the user-covariate is represented by CO_2 emissions over the US (Figure 5.a). Territorial fossil fuel CO_2 emissions data are available on Global Carbon Atlas `http://www.globalcarbonatlas.org/en/CO2-emissions` (Boden et al., 2017; BP, 2017; UNFCCC, 2017). To incorporate the observed relationship between temperature and CO_2 in the statistical model (Figure 5.b), we select a model in which the location and the scale parameters of the GEV distribution are linear
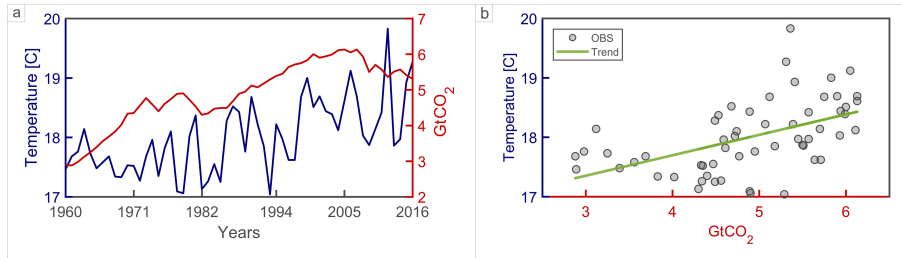
24

Figure 5: Application 2: Modeling temperature maxima with CO_2 emissions as the physical covariate. a) Temperature and CO_2 time series; b) Annual temperature maxima as a function of CO_2 emissions in the atmosphere

functions of the covariate, while the shape parameter is constant. We assume normal priors. Figure 6.b shows the results of the nonstationary model for a value of CO_2 equal to 4.9 $GtCO_2$. For comparison, we also plot the results when a stationary model is selected in Figure 6.a. One can see that the nonstationary model better captures the observed extreme events, particularly events associated with higher values of CO_2. Moreover, the diagnostics tests confirm that the nonstationary model is a better fit. For the nonstationary model, the AIC and the BIC are 93.91 and 104.13, respectively. When the stationary model is considered, both the AIC and BIC increase to 104.98 and 111.11, respectively. Lower values of AIC and BIC indicate a superior model performance. The advantage of the AIC and BIC for model selection is their ability to account for the number of model parameters: models with more parameters are penalized. Figure S1 shows the effective return level as a function of CO_2 emissions. The results show how temperature extremes change in response to the increasing CO_2 emissions (here, the physical covariate). For example, looking at the expected magnitude of a 50-year event, the temperature increases of about 4%, from 18.79 °C to 19.5 °C, when the CO_2 emissions increase from 4.49 $GtCO_2$ to 5.51 $GtCO_2$. The results are consistent with the expectation that higher CO_2 leads to a warmer climate, indicating that the statistical nonstationary model is able to model the observed physical relationship between temperature and CO_2.
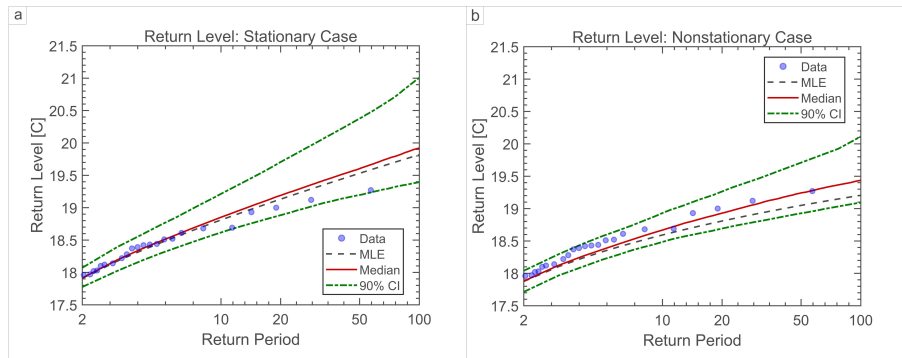
25

Figure 6: ProNEVA results for Application 2: Modeling temperature maxima with CO_2 emissions as the physical covariate. a) Return Level curves based on a stationary model; b) Return Level base on a nonstationary model considering CO_2 emissions equal to 4.9 $GtCO_2$.

9.3. Application 3: Modeling sea level rise with time as the covariate

The coastal city of Trieste (Italy) has been experiencing increasing sea level height over the years (Figure S2). Given the observed trend, we investigate annual maxima sea level data from the Permanent Service for Mean Sea Level (PSMSL - station ID 154) by adopting a temporal nonstationary GEV model. The purpose of this example is to show that ProNEVA can also be used for temporal nonstationary analysis. The location and scale parameters of the GEV distribution are modeled as linear functions of the time-covarite. The shape parameter is kept constant and we use normal priors for parameter estimation.

Figure 7.b shows the return level curves for a fixed value of the time-covariate equal to 45 years from the first observation (i.e., 45 years into the future from the beginning of the data). The nonstationary analysis in Figure 7.b provides better performance that the stationary model in Figure 7.a. Both the AIC and the BIC values confirm that the nonstationary model is the best choice to represent sea level observations in a changing climate. The AIC for the nonstationary model is 976.69, while it is 992.74 for the stationary model. Similarly, the BIC for the temporal nonstationary model is 989.08, while it is 1000 for the stationary model. Lower values for AIC and BIC indicates a superior model. The value of the temporal covariate should be regarded as the time at which
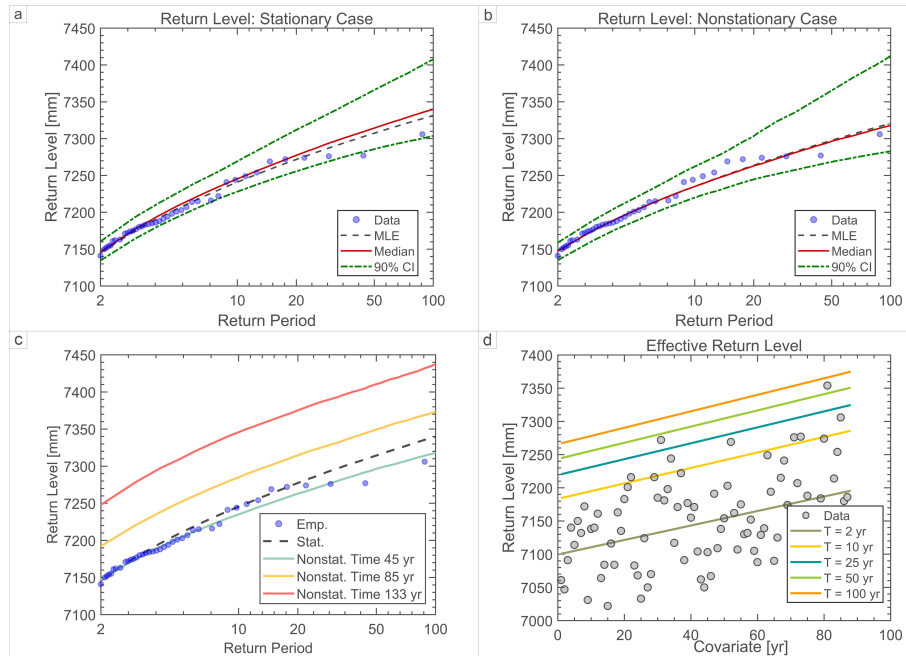
26

Figure 7: ProNEVA results for Application 3: Modeling sea level rise with time as the covariate. a) Return Level curves based on a stationary model; b) Return Level base on a nonstationary model considering equal to 45 years from the first observation; c) Expected return level curves, i.e. ensemble medians, under stationary and nonstationary assumption; d) Effective return period, i.e. return period as a function of the covariate, here time.

we estimate expected values of, as in this specific case, sea level. The expected (ensemble median) nonstationary return level curves in Figure 7.c refer to three different time at which we evaluate sea level: 45, 85, and 133 years from the first observation. Here, 133 years from the first observation is beyond the period of observations (88 years) meaning that we project into the future the observed trend and we infer from there. The observed increasing trend in the sea level records results in increasing values of sea level for higher value of the temporal covariate (Figure 7.c). For example, a 50 year event is equal to 7296.3 mm for time equal to 45 years from the first observation, 7349.3 mm for 85 years, and 7410.4 mm for 133 years. We register about 2% increase in sea level when the time of the first observation changes from 45 to 133 years, confirming the ability

27

of the nonstationary model to reproduce the increasing trend in observations. On the contrary, the stationary analysis returns a 50-year sea level equal to

₅₉₅ 7314.3 mm regardless of the first observation. Figure 7.d shows the effective return level curves, which capture the variability over time (here, the covariate) in the observed data. In the case of a nonstationary model with a temporal covariate, it is possible to evaluate the expected waiting time (Wigley, 2009; Olsen et al., 1998; Salas & Obeysekera, 2014), which incorporates the observed

₆₀₀ changes in the sea level over time in the estimation of return periods. Figure S3 shows that the current return periods (lower x-axis) will change considering the observed nonstationarity (upper x-asis). For example, the 100-year sea level estimated at t_0 (beginning of the simulation) turns into a 40-year event when the observed trend over time in sea level values is taken into account.

₆₀₅ *9.4. Application 4: Modeling precipitation under a stationary assumption*

This application focuses on the Generalized Pareto (GP) distribution for peak-over-threshold extreme value analysis. We investigate a time series of precipitation from New Orleans, Lousiana, that does not exhibit changes in statistics of extremes. We obtain daily precipitation from the National Climatic Data

₆₁₀ Center (NCDC) archive (`https://www.ncdc.noaa.gov/cdo-web/`) for the city of New Orleans, station GHCND:USW00012930. Given that we are interested in heavy precipitation events, we use a GP distribution to focus on values above a high threshold (i.e., avoid including non-extreme values). We extract precipitation excesses considering a constant threshold of the 98th-percentile of daily

₆₁₅ precipitation values (Figure S4).

For this application we select a stationary GP model, given that we do not have physical evidence to justify a more complex model. However, for the sake of comparison, we perform a nonstationary analysis considering the scale parameter as a linear function of time. Figure 8.a represents the return

₆₂₀ level curves based on a stationary model, while Figure 8.b depicts return level curves for a value of the covariate (here time) equal to half of the period of observation. From a comparison between the two models, the stationary model

28

performs better. The stationary model returns values of the AIC and BIC equal to 713.3 and 721.14, respectively. For the nonstationary model the values of the

₆₂₅ AIC and BIC are slightly higher (715.02 and 726.79, respectively). The results of this example application suggests that when no evidence of changes due to a physical process can be identified, ProNEVA favors the simplest form of model that represents the historical observations.
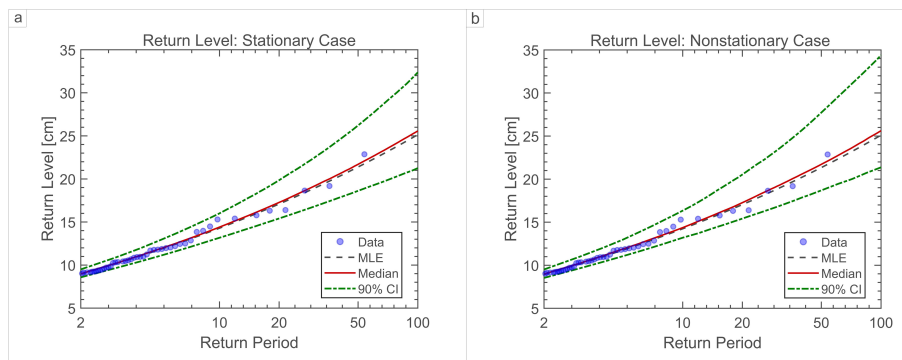

Figure 8: ProNEVA results for Application 4: Modeling precipitation under a stationary assumption. a) Return Level curves under the stationary assumption; b) Return Level curves under the temporal nonstationary assumption for a value of the covariate within the period of observation.

10. Conclusion

₆₃₀ The ability to reliably estimate the expected magnitude and frequency of extreme events is fundamental for improving design concepts and risk assessment methods. This is particularly important for extreme events that have significant impacts on society, infrastructure and human lives, such as extreme precipitation events causing flooding and landslides.

₆₃₅ The observed increase in extreme events and their impacts reported from around the world have motivated moving away from the so-called stationary approach to ensure capturing the changing properties of extremes (Milly et al., 2008). However, there are opposing opinions and perspective on the need and also form of suitable nonstationary models for extreme value analysis. Most of

the existing tools for implementing extreme value analysis under the nonstationary assumption have a number of limitations including lack of a generalized framework for incorporating physically based covariates and estimating parameters, which depend on a generic physical covariate. To address these limitations, we propose a generalized framework entitled *Process-informed Nonstationary Extreme Value Analysis* (ProNEVA) in which the nonstationarity component is defined by a temporal or physical-based dependence of the observed extremes on a physical driver (e.g., change in runoff in response to urbanization, or change in extreme temperatures in response to CO_2 emissions). ProNEVA offers stationary and temporal and process-informed nonstationary extreme value analysis, parameter estimation, uncertainty quantification, and a comprehensive assessment of the goodness of fit.

Here we applied ProNEVA to four different types of applications describing change in: extreme river discharge in response to urbanization, extreme sea levels over time, extreme temperatures in response to CO_2 emissions in the atmosphere. We have also demonstrated a peak-over-threshold approach using precipitation data. The results indicate that ProNEVA offers reliable estimates when considering a physical-process or time as a covriate.

The source code of ProNEVA is freely available to the scientific community. A graphical user inter face (GUI) version of the model, Figure 2, is also available to facilitate its applications (see Supporting Information). We hope that ProNEVA motivates more process-informed nonstationary analysis of extreme events.

Acknowledgments

available online. Links to the data are provided in the dedicated section. We

References

AghaKouchak, A., Feldman, D., Stewardson, M. J., Saphores, J.-D., Grant, S., & Sanders, B. F. (2014). Australia's Drought: Lessons for California. *Science*, *343*, 1430–1431.

Aho, K., Derryberry, D., & Peterson, T. (2014). Model selection for ecologists: the worldviews of AIC and BIC. *Ecology*, *95*, 631–636. URL: `http://www.jstor.org/stable/43495189`.

Akaike, H. (1974). A new look at the statistical model identification. *IEEE Transactions on Automatic Control*, *19*, 716–723. doi:`10.1109/TAC.1974.1100705`.

Akaike, H. (1998). Information Theory and an Extension of the Maximum Likelihood Principle BT - Selected Papers of Hirotugu Akaike. (pp. 199–213). New York, NY: Springer New York. URL: `https://doi.org/10.1007/978-1-4612-1694-0{_}15`. doi:`10.1007/978-1-4612-1694-0_15`.

Alexander, L. V., Zhang, X., Peterson, T. C., Caesar, J., Gleason, B., Klein Tank, A. M., Haylock, M., Collins, D., Trewin, B., Rahimzadeh, F., Tagipour, A., Rupa Kumar, K., Revadekar, J., Griffiths, G., Vincent, L., Stephenson, D. B., Burn, J., Aguilar, E., Brunet, M., Taylor, M., New, M., Zhai, P., Rusticucci, M., & Vazquez-Aguirre, J. L. (2006). Global observed changes in daily climate extremes of temperature and precipitation. *Journal of Geophysical Research Atmospheres*, *111*, 1–22. doi:`10.1029/2005JD006290`.

Barnett, T. P., Hasselmann, K., Chelliah, M., Delworth, T., Hegerl, G., Jones, P., Rasmusson, E., Roeckner, E., Ropelewski, C., Santer, B., & Tett, S. (1999). Detection and attribution of recent climate change: A status report. *Bulletin of the American Meteorological Society*, *80*, 2631–2659. doi:`10.1175/1520-0477(1999)080<2631:DAAORC>2.0.CO;2`.

Boden, T., Marland, G., & Andres, R. (2017). Global, Regional, and Nation al Fossil Fuel CO2 Emissions. Carbon Dioxide Information Analysis

⁷⁰⁰ Center. Oak Ridge National Laboratory, U.S. Department of Energy, Oak Ridge, Tenn., USA. http://cdiac.ess-dive.lbl.gov/trends/emis/meth_reg.html. URL: `http://cdiac.ess-dive.lbl.gov/trends/emis/meth{_}reg.html`. doi:`10.3334/CDIAC/00001_V2017`.

BP (2017). Statistical Review of World Energy.
⁷⁰⁵ http://www.bp.com/en/global/corporate/energy-economics.html, . URL: `http://www.bp.com/en/global/corporate/energy-economics.html`.

Bracken, C., Holman, K. D., Rajagopalan, B., & Moradkhani, H. (2018). A Bayesian Hierarchical Approach to Multivariate Nonstationary Hydrologic Frequency Analysis. *Water Resources Research*, (pp. 243–255). doi:`10.1002/`
⁷¹⁰ `2017WR020403`.

Cannon, A. J. (2010). A flexible nonlinear modelling framework for nonstationary generalized extreme value analysis in hydroclimatology. *Hydrological Processes*, *24*, 673–685. doi:`10.1002/hyp.7506`.

Cheng, L., & AghaKouchak, A. (2014). Nonstationary precipitation Intensity-
⁷¹⁵ Duration-Frequency curves for infrastructure design in a changing climate. *Scientific reports*, *4*, 7093. URL: `http://www.nature.com/srep/2014/141118/srep07093/full/srep07093.html`. doi:`10.1038/srep07093`.

Cheng, L., AghaKouchak, A., Gilleland, E., & Katz, R. W. (2014). Nonstationary extreme value analysis in a changing climate. *Climatic Change*,
⁷²⁰ *127*, 353–369. doi:`10.1007/s10584-014-1254-5`.

Coles, S., & Pericchi, L. (2003). Antecipating Catastrophes Through Extreme Value Modeling. *Journal of the Royal Statistical Society - Series C - Applied Statistics*, *52*, 405–416.

Coles, S. G. (2001). *An introduction to Statistical Modeling of Extreme Values*.
⁷²⁵ Springer. doi:`10.1007/978-1-4471-3675-0`.

Cooley, D. (2013). Return Periods and Return Levels Under Climate Change. In A. AghaKouchak, D. Easterling, K. Hsu, S. Schubert, & S. Sorooshian

(Eds.), *Extremes in a Changing Climate: Detection, Analysis and Uncertainty* chapter 4. (pp. 97–114). Dordrecht: Springer Netherlands.

Cooley, D., Nychka, D., & Naveau, P. (2007). Bayesian Spatial Modeling of Extreme Precipitation Return Levels. *Journal of the American Statistical Association*, *102*, 824–840. doi:`10.1198/016214506000000780`.

Coumou, D., & Rahmstorf, S. (2012). A decade of weather extremes. *Nature Climate Change*, *2*, 491–496. URL: `http://dx.doi.org/10.1038/nclimate1452`. doi:`10.1038/nclimate1452`.

De Michele, C., & Salvadori, G. (2003). A Generalized Pareto intensity-duration model of storm rainfall exploiting 2-Copulas. *Journal of Geophysical Research Atmospheres*, *108*, 1–11. doi:`10.1029/2002JD002534`.

Diffenbaugh, N. S., Swain, D. L., & Touma, D. (2015). Anthropogenic warming has increased drought risk in California. *Proceedings of the National Academy of Sciences*, *112*, 3931–3936. URL: `http://www.pnas.org/content/112/13/3931`.

Duan, Q. Y., Gupta, V. K., & Sorooshian, S. (1993). Shuffled complex evolution approach for effective and efficient global minimization. *Journal of Optimization Theory and Applications*, *76*, 501–521. URL: `https://doi.org/10.1007/BF00939380`. doi:`10.1007/BF00939380`.

Farajzadeh, M., Rahimi, M., Kamali, G. A., & Mavrommatis, T. (2010). Modelling apple tree bud burst time and frost risk in Iran. *Meteorological Applications*, *17*, 45–52. doi:`10.1002/met.159`.

Fischer, E. M., & Knutti, R. (2015). Anthropogenic contribution to global occurrence of heavy-precipitation and high-temperature extremes. *Nature Clim. Change*, *5*, 560–564. URL: `http://dx.doi.org/10.1038/nclimate2617`.

Fischer, E. M., & Knutti, R. (2016). Observed heavy precipitation increase confirms theory and early models. *Nature Climate Change*, *6*, 986–

991. URL: http://www.nature.com/doifinder/10.1038/nclimate3110. doi:10.1038/nclimate3110.

Gelman, A., & Rubin, D. B. (1992). Inference from iterative simulation using multiple sequences. *Statist. Sci.*, *7*, 457–472. URL: https://doi.org/10.1214/ss/1177011136. doi:10.1214/ss/1177011136.

Gençay, R., & Selçuk, F. (2004). Extreme value theory and Value-at-Risk: Relative performance in emerging markets. *International Journal of Forecasting*, *20*, 287–303. URL: http://www.sciencedirect.com/science/article/pii/S0169207003001031. doi:https://doi.org/10.1016/j.ijforecast.2003.09.005.

Gilks, W., Roberts, G., & George, E. (1994). Adaptive Direction Sampling. *Journal of the Royal Statistical Society. Series D (The Statistician)*, *43*, 179–189. URL: http://www.jstor.org/stable/2348942. doi:10.2307/2348942.

Gilleland, E., & Katz, R. W. (2016). extRemes 2.0: An Extreme Value Analysis Package in <i>R</i>. *Journal of Statistical Software*, *72*. URL: http://www.jstatsoft.org/v72/i08/. doi:10.18637/jss.v072.i08.

Gilleland, E., Ribatet, M., & Stephenson, A. G. (2013). A software review for extreme value analysis. *Extremes*, *16*, 103–119. doi:10.1007/s10687-012-0155-0. arXiv:arXiv:1011.1669v3.

Griffis, V. W., Asce, M., Stedinger, J. R., & Asce, M. (2007). Log-Pearson Type 3 Distribution and Its Application in Flood Frequency Analysis . I : Distribution Characteristics. *Journal of Hydrologic Engineering*, *12*, 482–491.

Griffis, V. W., & Stedinger, J. R. (2007). Incorporating Climate Change and Variability into Bulletin 17B LP3 Model. URL: https://doi.org/10.1061/40927(243)69. doi:doi:10.1061/40927(243)69.

35

Gupta, H. V., Wagener, T., & Liu, Y. (2008). Reconciling theory with observations: elements of a diagnostic approach to model evaluation. *Hydrological Processes*, *22*, 3802–3813. doi:`10.1002/hyp`. arXiv:`arXiv:1011.1669v3`.

Gupta, I. D., & Deshpande, V. C. (1994). Application of Log-Pearson Type-3 Distribution for Evaluation of Design Earthquake Magnitude. *Journal of the Institution of Engineers (India), Civil Engineering Division*, *75*, 129–134.

Haario, H., Saksman, E., & Tamminen, J. (1999). Adaptive proposal distribution for random walk Metropolis algorithm. *Computational Statistics*, *14*, 375–395. URL: `https://doi.org/10.1007/s001800050022`. doi:`10.1007/s001800050022`.

Haario, H., Saksman, E., & Tamminen, J. (2001). An adaptive Metropolis algorithm. *Bernoulli*, *7*, 223–242. URL: `https://projecteuclid.org:443/euclid.bj/1080222083`.

Haigh, I., Nicholls, R., & Wells, N. (2010). Assessing changes in extreme sea levels: Application to the English Channel, 1900-2006. *Continental Shelf Research*, *30*, 1042–1055. URL: `http://dx.doi.org/10.1016/j.csr.2010.02.002`. doi:`10.1016/j.csr.2010.02.002`.

Hallegatte, S., Green, C., Nicholls, R. J., & Corfee-Morlot, J. (2013). Future flood losses in major coastal cities. *Nature Climate Change*, *3*, 802–806. doi:`10.1038/nclimate1979`. arXiv:`arXiv:1011.1669v3`.

Holgate, S. J. (2007). On the decadal rates of sea level change during the twentieth century. *Geophysical Research Letters*, *34*, 2001–2004. doi:`10.1029/2006GL028492`.

Holmes, J. D., & Moriarty, W. W. (1999). Application of the generalized Pareto distribution to extreme value analysis in wind engineering. *Journal of Wind Engineering and Industrial Aerodynamics*, *83*, 1–10. URL: `http://www.sciencedirect.com/science/article/`

pii/S0167610599000562. doi:https://doi.org/10.1016/S0167-6105(99)00056-2.

Huard, D., Mailhot, A., & Duchesne, S. (2009). Bayesian estimation of intensity-duration-frequency curves and of the return period associated to a given rainfall event. *Stochastic Environmental Research and Risk Assessment*, *24*, 337–347. doi:10.1007/s00477-009-0323-1.

Hurkmans, R. T. W. L., Terink, W., Uijlenhoet, R., Moors, E. J., Troch, P. A., & Verburg, P. H. (2009). Effects of land use changes on streamflow generation in the Rhine basin. *Water Resources Research*, *45*, 1–15. doi:10.1029/2008WR007574.

Jongman, B., Hochrainer-Stigler, S., Feyen, L., Aerts, J. C. J. H., Mechler, R., Botzen, W. J. W., Bouwer, L. M., Pflug, G., Rojas, R., & Ward, P. J. (2014). Increasing stress on disaster-risk finance due to large floods. *Nature Climate Change*, *4*, 264–268. doi:10.1038/nclimate2124. arXiv:nclimate2124.

Katz, R. W. (2013). Statistical Methods for Nonstationary Extremes. In A. AghaKouchak, D. Easterling, K. Hsu, S. Schubert, & S. Sorooshian (Eds.), *Extremes in a Changing Climate: Detection, Analysis and Uncertainty* (pp. 15–37). Dordrecht: Springer Netherlands. doi:10.1007/978-94-007-4479-0{_}2.

Katz, R. W., Parlange, M. B., & Naveau, P. (2002). Statistics of extremes in hydrology. *Advances in Water Resources*, *25*, 1287–1304. URL: http://www.sciencedirect.com/science/article/pii/S0309170802000568?via{%}3Dihub. doi:10.1016/S0309-1708(02)00056-8.

Klemeš, V. (1974). The Hurst Phenomenon: A puzzle? *Water Resources Research*, *10*, 675–688. doi:10.1029/WR010i004p00675.

Koenker, R., & Bassett, G. J. (1978). Regression Quantiles. *Econometrica*, *46*, 33–50.

Koutrouvelis, I. A., & Canavos, G. C. (1999). Estimation in the Pearson type 3 distribution. *Water Resources Research*, *35*, 2693–2704. URL: `http://dx.doi.org/10.1029/1999WR900174`. doi:`10.1029/1999WR900174`.

Koutsoyiannis, D. (2011). Hurst-Kolmogorov Dynamics and Uncertainty. *Journal of the American Water Resources Association*, *47*, 481–495. doi:`10.1111/j.1752-1688.2011.00543.x`.

Koutsoyiannis, D., & Montanari, A. (2007). Statistical analysis of hydroclimatic time series: Uncertainty and insights. *Water Resources Research*, *43*, 1–9. doi:`10.1029/2006WR005592`.

Koutsoyiannis, D., & Montanari, A. (2015). Negligent killing of scientific concepts: the stationary case. *Hydrological Sciences Journal*, *60*, 1174–1183. URL: `http://dx.doi.org/10.1080/02626667.2014.959959`. doi:`10.1080/02626667.2014.959959`.

Krishnaswamy, J., Vaidyanathan, S., Rajagopalan, B., Bonell, M., Sankaran, M., Bhalla, R. S., & Badiger, S. (2015). Non-stationary and non-linear influence of ENSO and Indian Ocean Dipole on the variability of Indian monsoon rainfall and extreme rain events. *Climate Dynamics*, *45*, 175–184. doi:`10.1007/s00382-014-2288-0`.

Kwon, H. H., & Lall, U. (2016). A copula-based nonstationary frequency analysis for the 2012-2015 drought in California. *Water Resources Research*, *52*, 5662–5675. doi:`10.1002/2016WR018959`. arXiv:`2014WR016527`.

Kyselý, J., Picek, J., & Beranová, R. (2010). Estimating extremes in climate change simulations using the peaks-over-threshold method with a non-stationary threshold. *Global and Planetary Change*, *72*, 55–68. URL: `http://dx.doi.org/10.1016/j.gloplacha.2010.03.006`. doi:`10.1016/j.gloplacha.2010.03.006`.

Lima, C. H., Lall, U., Troy, T., & Devineni, N. (2016a). A hierarchical bayesian gev model for improving local and regional flood quan-

38

tile estimates. *Journal of Hydrology*, *541*, 816 – 823. URL: `http://www.sciencedirect.com/science/article/pii/S0022169416304723`.

doi:`https://doi.org/10.1016/j.jhydrol.2016.07.042`.

Lima, C. H., Lall, U., Troy, T. J., & Devineni, N. (2015). A climate informed model for nonstationary flood risk prediction: Application to negro river at manaus, amazonia. *Journal of Hydrology*, *522*, 594 – 602. URL: `http://www.sciencedirect.com/science/article/pii/S0022169415000153`. doi:`https://doi.org/10.1016/j.jhydrol.2015.01.009`.

Lima, C. H. R., Kwon, H.-H., & Kim, J.-Y. (2016b). A Bayesian beta distribution model for estimating rainfall IDF curves in a changing climate. *Journal of Hydrology*, *540*, 744–756. URL: `http://www.sciencedirect.com/science/article/pii/S0022169416304243`. doi:`https://doi.org/10.1016/j.jhydrol.2016.06.062`.

Lins, H. F., & Cohn, T. A. (2011). Stationarity: Wanted dead or alive? *Journal of the American Water Resources Association*, *47*, 475–480. doi:`10.1111/j.1752-1688.2011.00542.x`.

Luke, A., Vrugt, J. A., AghaKouchak, A., Matthew, R., & Sanders, B. F. (2017). Predicting nonstationary flood frequencies: Evidence supports an updated stationarity thesis in the United States. *Water Resources Research*, *53*, 5469–5494. URL: `http://dx.doi.org/10.1002/2016WR019676`. doi:`10.1002/2016WR019676`.

Madsen, H., Lawrence, D., Lang, M., Martinkova, M., & Kjeldsen, T. (2013). A review of applied methods in europe for flood-frequency analysis in a changing environment, .

Mailhot, A., Duchesne, S., Caya, D., & Talbot, G. (2007). Assessment of future change in intensity-duration-frequency (IDF) curves for Southern Quebec using the Canadian Regional Climate Model (CRCM). *Journal of Hydrology*, *347*, 197–210. doi:`10.1016/j.jhydrol.2007.09.019`.

Mallakpour, I., & Villarini, G. (2017). Analysis of changes in the magnitude, frequency, and seasonality of heavy precipitation over the contiguous USA. *Theoretical and Applied Climatology*, *130*, 345–363. doi:`10.1007/s00704-016-1881-z`.

Marvel, K., & Bonfils, C. (2013). Identifying external influences on global precipitation. *Proceedings of the National Academy of Sciences*, *110*, 19301–19306. URL: `http://www.pnas.org/content/112/13/3931`. doi:`10.1073/pnas.1314382110`.

Massey, F. J. J. (1951). Kolmogorov-Smirnov Test for Goodness of Fit. *Journal of the American Statistical Association*, *46*, 68– 78. doi:`10.1080/01621459.1951.10500769`. arXiv:`dfg`.

Matalas, N. C. (1997). Stochastic hydrology in the context of climate change. doi:`10.1023/A:1005374000318`.

Matalas, N. C. (2012). Comment on the Announced Death of Stationarity. *Journal of Water Resources Planning and Management*, *138*, 311–312. URL: `http://ascelibrary.org/doi/10.1061/{%}28ASCE{%}29WR.1943-5452.0000215`. doi:`10.1061/(ASCE)WR.1943-5452.0000215`.

Mazdiyasni, O., & AghaKouchak, A. (2015). Substantial increase in concurrent droughts and heatwaves in the United States. *Proceedings of the National Academy of Sciences*, *112*, 11484–11489. URL: `http://www.pnas.org/lookup/doi/10.1073/pnas.1422945112`. doi:`10.1073/pnas.1422945112`.

Mazdiyasni, O., Aghakouchak, A., Davis, S. J., Madadgar, S., Mehran, A., Ragno, E., Sadegh, M., Sengupta, A., Ghosh, S., Dhanya, C. T., & Niknejad, M. (2017). Increasing probability of mortality during Indian heat waves. *Science Advances*, (pp. 1–6).

Melillo, J. M., Richmond, T. T., & Yohe, G. W. (2014). *Climate Change Impacts in the United States*. URL: `http://nca2014.globalchange.gov/downloads`. doi:`10.7930/J01Z429C.On`.

Mentaschi, L., Vousdoukas, M., Voukouvalas, E., Sartini, L., Feyen, L., Besio, G., & Alfieri, L. (2016). The transformed-stationary approach: a generic and simplified methodology for non-stationary extreme value analysis. *Hydrology and Earth System Sciences*, *20*, 3527–3547. URL: http://www.hydrol-earth-syst-sci.net/20/3527/2016/. doi:10.5194/hess-20-3527-2016.

Milly, P. C. D., Betancourt, J., Falkenmark, M., Hirsch, R. M., Kundzewicz, Z. W., Lettenmaier, D. P., & Stouffer, R. J. (2008). Stationarity is dead: whither water management? *Science (New York, N.Y.)*, *319*, 573–574. doi:10.1126/science.1151915. arXiv:science.1151915.

Min, S.-K., Zhang, X., Zwiers, F. W., & Hegerl, G. C. (2011). Human contribution to more-intense precipitation extremes. *Nature*, *470*, 378–381. URL: http://www.ncbi.nlm.nih.gov/pubmed/21331039. doi:10.1038/nature09763.

Ming, L., M., F. D., & Sunyong, K. (2009). Bridge System Performance Assessment from Structural Health Monitoring: A Case Study. *Journal of Structural Engineering*, *135*, 733–742. URL: https://doi.org/10.1061/(ASCE)ST.1943-541X.0000014. doi:10.1061/(ASCE)ST.1943-541X.0000014.

Mirhosseini, G., Srivastava, P., & Fang, X. (2014). Developing Rainfall Intensity-Duration-Frequency (IDF) Curves for Alabama under Future Climate Scenarios using Artificial Neural Network (ANN). *Journal of Hydrologic Engineering*, *04014022*, 1–10. URL: http://ascelibrary.org/doi/abs/10.1061/(ASCE)HE.1943-5584.0000962. doi:10.1061/(ASCE)HE.1943-5584.0000962.

Mirhosseini, G., Srivastava, P., & Sharifi, A. (2015). Developing Probability-Based IDF Curves Using Kernel Density Estimator. *Journal of Hydrologic Engineering*, *20*. URL: http://www.scopus.com/inward/record.url?eid=2-s2.0-84939224959{&}partnerID=tZOtx3y1. doi:10.1061/(ASCE)HE.1943-5584.0001160.

Mondal, A., & Mujumdar, P. (2015). Modeling non-stationarity in intensity, duration and frequency of extreme rainfall over India. *Journal of Hydrology*, *521*, 217–231. URL: `http://www.sciencedirect.com/science/article/pii/S0022169414009937`. doi:`10.1016/j.jhydrol.2014.11.071`.

Montanari, A., & Koutsoyiannis, D. (2014). Modeling and mitigating natural hazards: Stationary is immortal! *Water resources research*, *50*, 9748–9756. doi:`10.1002/2014WR016092.Received`.

Obeysekera, J., & Salas, J. D. (2013). Quantifying the Uncertainty of Design Floods Under Non-Stationary Conditions. *Journal of Hydrologic Engineering*, *19*, 1438–1446. URL: `http://ascelibrary.org/doi/abs/10.1061/(ASCE)HE.1943-5584.0000931`. doi:`10.1061/(ASCE)HE.1943-5584.0000931`.

Olsen, J. R., Lambert, J. H., & Haimes, Y. Y. (1998). Risk of extreme events under nonstationary conditions. *Risk Analysis*, *18*, 497–510. doi:`10.1111/j.1539-6924.1998.tb00364.x`.

Papalexiou, S. M., & Koutsoyiannis, D. (2013). Battle of extreme value distributions : A global survey on extreme daily rainfall. *Water Resources Research*, *49*, 187–201. doi:`10.1029/2012WR012557`.

Pisarenko, V. F., & Sornette, D. (2003). Characterization of the Frequency of Extreme Earthquake Events by the Generalized Pareto Distribution. *pure and applied geophysics*, *160*, 2343–2364. URL: `https://doi.org/10.1007/s00024-003-2397-x`. doi:`10.1007/s00024-003-2397-x`.

Ragno, E., AghaKouchak, A., Love, C. A., Cheng, L., Vahedifard, F., & Lima, C. H. R. (2018). Quantifying Changes in Future Intensity-Duration-Frequency Curves Using Multi-Model Ensemble Simulations. *Water Resources Research*, (pp. 1–38). URL: `http://doi.wiley.com/10.1002/2017WR021975`. doi:`10.1002/2017WR021975`.

Read, L. K., & Vogel, R. M. (2015). Reliability, return periods, and risk under

nonstationarity. *Water Resources Research*, *51*, 6381–6398. doi:`10.1002/` `2014WR016259`. arXiv:`2014WR016527`.

Renard, B., Sun, X., & Lang, M. (2013). Bayesian Methods for Non-stationary Extreme Value Analysis. In A. AghaKouchak, D. Easterling, K. Hsu, S. Schubert, & S. Sorooshian (Eds.), *Extremes in a Changing Climate: Detection, Analysis and Uncertainty* (pp. 39–95). Dordrecht: Springer Netherlands. URL: `https://doi.org/10.1007/978-94-007-4479-0{_}3`. doi:`10.1007/978-94-007-4479-0_3`.

Roberts, G. O., & Rosenthal, J. S. (2009). Examples of Adaptive MCMC. *Journal of Computational and Graphical Statistics*, *18*, 349–367. URL: `http://www.jstor.org/stable/25651249`.

Roberts, G. O., & Sahu, S. K. (1997). Updating Schemes, Correlation Structure, Blocking and Parameterization for the Gibbs Sampler. *Journal of the Royal Statistical Society: Series B (Statistical Methodology)*, *59*, 291–317. URL: `http://dx.doi.org/10.1111/1467-9868.00070`. doi:`10.1111/1467-9868.00070`.

Rosner, A., Vogel, R. M., & Kirshen, P. H. (2014). A risk-based approach to flood management decisions in a nonstationary world. *Water Resources Research*, *50*, 1928 – 1942. URL: `http://dx.doi.org/10.1002/2013WR014561`. doi:`10.1002/2013WR014561.Received`.

Sadegh, M., Moftakhari, H., Gupta, H. V., Ragno, E., Mazdiyasni, O., Sanders, B., Matthew, R., & AghaKouchak, A. (2018). Multi-hazard scenarios for analysis of compound extreme events. *Geophysical Research Letters*, .

Sadegh, M., Ragno, E., & Aghakouchak, A. (2017). Multivariate Copula Analysis Toolbox (MvCAT): Describing dependence and underlying uncertainty using a Bayesian framework. *Water Resources Research*, (pp. 1–18). doi:`10.1002/2016WR020242`.

Sadegh, M., & Vrugt, J. A. (2014). Approximate bayesian computation using markov chain monte carlo simulation: Dream (abc). *Water Resources Research*, *50*, 6767–6787.

Sadegh, M., Vrugt, J. A., Xu, C., & Volpi, E. (2015). The stationarity paradigm revisited: Hypothesis testing using diagnostics, summary metrics, and DREAM(ABC). *Water Resources Research*, *51*, 9207–9231. URL: `http://dx.doi.org/10.1002/2014WR016805`. doi:`10.1002/2014WR016805`.

Salas, J., Obeysekera, J., & Vogel, R. (2018). Techniques for assessing water infrastructure for nonstationary extreme events: a review. *Hydrological Sciences Journal*, *00*, 02626667.2018.1426858. URL: `https://www.tandfonline.com/doi/full/10.1080/02626667.2018.1426858`. doi:`10.1080/02626667.2018.1426858`.

Salas, J. D., & Obeysekera, J. (2014). Revisiting the Concepts of Return Period and Risk for Nonstationary Hydrologic Extreme Events. *Journal of Hydrologic Engineering*, (pp. 554–568). doi:`10.1061/(ASCE)HE.1943-5584.0000820`.

Salas, J. D., & Pielke Sr, R. A. (2002). Stochastic characteristics and modeling of hydroclimatic processes. *Handbook of Weather, Climate, and Water*, (pp. 585–603).

Salas, J. D., Rajagopalan, B., Saito, L., & Brown, C. (2012). Special section on climate change and water resources: Climate nonstationarity and water resources management. *Journal of Water Resources Planning and Management*, *138*, 385–388. doi:`doi:10.1061/(ASCE)WR.1943-5452.0000279`.

Sankarasubramanian, A., & Lall, U. (2003). Flood quantiles in a changing climate: Seasonal forecasts and causal relations. *Water Resources Research*, *39*. URL: `http://dx.doi.org/10.1029/2002WR001593`. doi:`10.1029/2002WR001593`.

Sarhadi, A., Burn, D. H., Concepción Ausín, M., & Wiper, M. P. (2016). Time-varying nonstationary multivariate risk analysis using a dynamic Bayesian

copula. *Water Resources Research*, *52*, 2327–2349. URL: `http://dx.doi.org/10.1002/2015WR018525`. doi:`10.1002/2015WR018525`.

Sarhadi, A., & Soulis, E. D. (2017). Time-varying extreme rainfall intensity-duration-frequency curves in a changing climate. *Geophysical Research Letters*, (pp. 1–10). URL: `http://doi.wiley.com/10.1002/2016GL072201`. doi:`10.1002/2016GL072201`.

Schwarz, G. (1978). Estimating the Dimension of a Model. *Ann. Statist.*, *6*, 461–464. URL: `https://projecteuclid.org:443/euclid.aos/1176344136`. doi:`10.1214/aos/1176344136`.

Serago, J. M., & Vogel, R. M. (2018). Parsimonious nonstationary flood frequency analysis. *Advances in Water Resources*, *112*, 1–16. doi:`10.1016/j.advwatres.2017.11.026`.

Serinaldi, F., & Kilsby, C. G. (2015). Stationarity is undead: Uncertainty dominates the distribution of extremes. *Advances in Water Resources*, *77*, 17–36. URL: `http://dx.doi.org/10.1016/j.advwatres.2014.12.013`. doi:`10.1016/j.advwatres.2014.12.013`.

Stahl, K., Hisdal, H., Hannaford, J., Tallaksen, L. M., Van Lanen, H. A., Sauquet, E., Demuth, S., Fendekova, M., & Jodar, J. (2010). Streamflow trends in Europe: Evidence from a dataset of near-natural catchments. *Hydrology and Earth System Sciences*, *14*, 2367–2382. doi:`10.5194/hess-14-2367-2010`.

Steinschneider, S., & Lall, U. (2015). A hierarchical bayesian regional model for nonstationary precipitation extremes in northern california conditioned on tropical moisture exports. *Water Resources Research*, *51*, 1472–1492. URL: `https://agupubs.onlinelibrary.wiley.com/doi/abs/10.1002/2014WR016664`. doi:`10.1002/2014WR016664`. arXiv:`https://agupubs.onlinelibrary.wiley.com/doi/pdf/10.1002/2014WR016664`.

Storn, R., & Price, K. (1997). Differential Evolution – A Simple and Efficient Heuristic for global Optimization over Continuous Spaces. *Journal of Global Optimization*, *11*, 341–359. URL: `https://doi.org/10.1023/A:1008202821328`. doi:`10.1023/A:1008202821328`.

Stott, P. A., Gillett, N. P., Hegerl, G. C., Karoly, D. J., Stone, D. A., Zhang, X., & Zwiers, F. (2010). Detection and attribution of climate change: a regional perspective. *Wiley Interdisciplinary Reviews: Climate Change*, *1*, 192–211. URL: `http://dx.doi.org/10.1002/wcc.34`. doi:`10.1002/wcc.34`.

Ter Braak, C. J. F., & Vrugt, J. A. (2008). Differential Evolution Markov Chain with snooker updater and fewer chains. *Statistics and Computing*, *18*, 435–446. URL: `https://doi.org/10.1007/s11222-008-9104-9`. doi:`10.1007/s11222-008-9104-9`.

Thiemann, M., Trosset, M., Gupta, H., & Sorooshian, S. (2001). Bayesian recursive parameter estimation for hydrologic models Water Resources Research Volume 37, Issue 10. *Water Resources Research*, *37*, 2521–2535. URL: `http://onlinelibrary.wiley.com/doi/10.1029/2000WR900405/abstract`. doi:`10.1029/2000WR900405`.

Towler, E., Rajagopalan, B., Gilleland, E., Summers, R. S., Yates, D., & Katz, R. W. (2010). Modeling hydrologic and water quality extremes in a changing climate: A statistical approach based on extreme value theory. *Water Resources Research*, *46*. URL: `https://agupubs.onlinelibrary.wiley.com/doi/abs/10.1029/2009WR008876`. doi:`10.1029/2009WR008876`. arXiv:`https://agupubs.onlinelibrary.wiley.com/doi/pdf/10.1029/2009WR008876`.

UNFCCC (2017). National Inventory Submissions. United Nations Framework Convention on Climate Change. URL: `http://unfccc.int/national{_}reports/annex{_}i{_}ghg{_}inventories/national{_}inventories{_}submissions/items/9492.php`.

U.S. Water Resources Council (1982). Guidelines for Determining Flood Flow

Frequency. *Bulletin 17B: Reston, Virginia, Hydrology Subcommittee, Office of Water Data Coordination, U.S. Geological Survey*, (p. 182).

Vahedifard, F., Robinson, J. D., & AghaKouchak, A. (2016). Can Protracted Drought Undermine the Structural Integrity of California's Earthen Levees? *Journal of Geotechnical and Geoenvironmental Engineering*, *142*, 02516001. URL: `http://ascelibrary.org/doi/10.1061/(ASCE)GT.1943-5606.0001465`. doi:`10.1061/(ASCE)GT.1943-5606.0001465`.

Villarini, G., Serinaldi, F., Smith, J. A., & Krajewski, W. F. (2009a). On the stationarity of annual flood peaks in the continental United States during the 20th century. *Water Resources Research*, *45*, 1–17. doi:`10.1029/2008WR007645`.

Villarini, G., Smith, J. A., & Napolitano, F. (2010). Nonstationary modeling of a long record of rainfall and temperature over Rome. *Advances in Water Resources*, *33*, 1256–1267. URL: `http://www.sciencedirect.com/science/article/pii/S030917081000062X`. doi:`https://doi.org/10.1016/j.advwatres.2010.03.013`.

Villarini, G., Smith, J. A., Serinaldi, F., Bales, J., Bates, P. D., & Krajewski, W. F. (2009b). Flood frequency analysis for nonstationary annual peak records in an urban drainage basin. *Advances in Water Resources*, *32*, 1255–1266. doi:`10.1016/j.advwatres.2009.05.003`.

Vogel, R. M., Yaindl, C., & Walter, M. (2011). Nonstationarity: Flood Magnification and Recurrence Reduction Factors in the United States. *JAWRA Journal of the American Water Resources Association*, *47*, 464–474. URL: `http://dx.doi.org/10.1111/j.1752-1688.2011.00541.x`. doi:`10.1111/j.1752-1688.2011.00541.x`.

Volpi, E., Fiori, A., Grimaldi, S., Lombardo, F., & Koutsoyiannis, D. (2015). One hundred years of return period: Strengths and limitations. *Water Resources Research*, *51*, 8570–8585. doi:`10.1002/2015WR017820`.

Vrugt, J., Ter Braak, C., Diks, C., Robinson, B., Hyman, J., & Hingdon, D. (2009). Accelerating Markov Chain Monte Carlo Simulation by Differential Evolution with Self-Adaptive Randomized Subspace Sampling. URL: `https://www.degruyter.com/view/j/ijnsns.2009.10.3/ijnsns.2009.10.3.273/ijnsns.2009.10.3.273.xml`. doi:`10.1515/IJNSNS.2009.10.3.273`.

Wahl, T., Jain, S., Bender, J., Meyers, S. D., & Luther, M. E. (2015). Increasing risk of compound flooding from storm surge and rainfall for major US cities. *Nature Clim. Change*, *5*, 1093–1097.

Wahl, T., Jensen, J., Frank, T., & Haigh, I. D. (2011). Improved estimates of mean sea level changes in the German Bight over the last 166 years. *Ocean Dynamics*, *61*, 701–715. doi:`10.1007/s10236-011-0383-x`.

Westra, S., Alexander, L. V., & Zwiers, F. W. (2013). Global Increasing Trends in Annual Maximum Daily Precipitation. *Journal of Climate*, *26*, 3904–3918. doi:`10.1175/JCLI-D-12-00502.1`.

Wigley, T. M. (2009). The effect of changing climate on the frequency of absolute extreme events. *Climatic Change*, *97*, 67–76. doi:`10.1007/s10584-009-9654-7`.

Willems, P., Arnbjerg-Nielsen, K., Olsson, J., & Nguyen, V. T. V. (2012). Climate change impact assessment on urban rainfall extremes and urban drainage: Methods and shortcomings. *Atmospheric Research*, *103*, 106–118. URL: `http://dx.doi.org/10.1016/j.atmosres.2011.04.003`. doi:`10.1016/j.atmosres.2011.04.003`.

Yan, H., Sun, N., Wigmosta, M., Skaggs, R., Hou, Z., & Leung, R. (2018). Next-Generation Intensity-Duration-Frequency Curves for Hydrologic Design in Snow-Dominated Environments. *Water Resources Research*, (pp. 1–16). URL: `http://doi.wiley.com/10.1002/2017WR021290`. doi:`10.1002/2017WR021290`.

Yilmaz, A. G., & Perera, B. J. C. (2014). Extreme Rainfall Nonstationarity Investigation and Intensity-Frequency-Duration Relationship. *Journal of Hydrologic Engineering*, *19*, 1160–1172. doi:`10.1061/(ASCE)HE.1943-5584.`
₁₁₄₅ `0000878`.

Zhang, X., Zwiers, F. W., Hegerl, G. C., Lambert, F. H., Gillett, N. P., Solomon, S., Stott, P. A., & Nozawa, T. (2007). Detection of human influence on twentieth-century precipitation trends. *Nature*, *448*, 461–465. URL: `http://dx.doi.org/10.1038/nature06025`.

₁₁₅₀ Zhang, X., Zwiers, F. W., & Stott, P. A. (2006). Multimodel Multisignal Climate Change Detection at Regional Scale. *Journal of Climate*, *19*, 4294–4307. doi:`10.1175/JCLI3851.1`.

Zhu, J., Stone, M. C., & Forsee, W. (2012). Analysis of potential impacts of climate change on Intensity - Duration - Frequency (IDF) relationships for six ₁₁₅₅ regions in the United States. *Journal of Water and Climate Change*, *3*, 185–196. URL: `http://jwcc.iwaponline.com/content/3/3/185`. doi:`10.2166/wcc.2012.045`.

Zwiers, F. W., Zhang, X., & Feng, Y. (2011). Anthropogenic Influence on Long Return Period Daily Temperature Extremes at Regional Scales. *Journal of* ₁₁₆₀ *Climate*, *24*, 881–892. doi:`10.1175/2010JCLI3908.1`.